



Novel anti-HIV cyclotriazadisulfonamide derivatives as modeled by ligand- and receptor-based approaches

Júlia R. Pinheiro, Michelle Bitencourt, Elaine F. F. da Cunha,*
Teodorico C. Ramalho* and Matheus P. Freitas*

Departamento de Química, Universidade Federal de Lavras, CP 3037, 37200-000, Lavras, MG, Brazil

Received 19 September 2007; revised 5 November 2007; accepted 7 November 2007

Available online 13 November 2007

Abstract—Computer-aided prediction of new anti-HIV compounds, derived from substructures of 2-amino-6-arylsulfonylbenzonitriles and cyclotriazadisulfonamide analogues, has been reported. A ligand-based approach, namely MIA-QSAR, and a docking evaluation were used to model the title compounds, macrocycles containing a trisubstituted benzene moiety. According to the MIA-QSAR method, predicted potencies for proposed compounds were up to seven times higher than that of the experimentally most active compound of training set. Moreover, we have used docking approaches to study the binding orientations and predict binding affinities of these compounds in CD4 receptor.

© 2007 Elsevier Ltd. All rights reserved.

1. Introduction

The acquired immunodeficiency syndrome (AIDS) epidemic has claimed about three million lives in 2006, and an estimated 4.3 million people have acquired the human immunodeficiency virus (HIV) in 2006, bringing to nearly 40 million the number of people globally living with the virus.¹ These alarming numbers have instigated the scientific community to search for therapies in the treatment of HIV-positive patients, and the development of novel and potent inhibitors for the treatment of HIV-1 infection has become the main focus in this field.

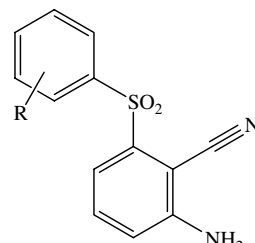
Garg et al.² have reviewed different classes of anti-HIV drugs, as well as the life cycle of HIV, which starts with the high-affinity binding of viral glycoprotein 120 (gp120) to CD4 receptor on the host cell surface. Inhibition of gp120 binding may be drawn by truncating the CD4 molecule. Other class of anti-HIV drugs is the HIV reverse transcriptase inhibitors. HIV records RNA into DNA using a key enzyme, reverse transcrip-

tase. Blocking this step has been used to prevent the virus replication.^{3,4} HIV protease, enzyme responsible for the fragmentation of protein chains to allow construction of new viral particles of HIV, is also an important target for the therapeutic class of protease inhibitors, such as ritonavir.⁵

Biologists, chemists and researchers in general are uninterruptedly looking for new entities having high potency against the HIV virus. Such ligands may be properly developed using computer-assisted methods, known as in silico QSAR (quantitative structure–activity relationship) procedures, which may be classified as ligand- and receptor-based approaches. The former is usually considered as a technique capable to manipulate a great amount of information (descriptors) in order to correlate bioactivities with the corresponding compounds. Great advances have occurred in this field since the classical Free-Wilson⁶ and Hansch⁷ methods for QSAR analysis. Nowadays, a variety of descriptors⁸ and three/multidimensional methods^{9–14} have been extensively applied to give highly predictive models to be used in drug design. In addition, the recently implemented MIA-QSAR method,^{15,16} whose descriptors derive from 2D images of chemical structures, has also provided important insights about drug discovery. Furthermore, receptor-based approaches, which are based on docking studies, have given useful information about ligand–receptor interactions. Consequently, the ligand affinity

Keywords: Anti-HIV compounds; CD4 receptor; MIA-QSAR; Docking studies.

* Corresponding authors. Tel.: +55 35 3829 1891; fax: +55 35 3829 1271 (M.P.F.); e-mail addresses: elaine_cunha@ufla.br; teo@ufla.br; matheus@ufla.br

Table 1. 2-Amino-6-arylsulfonylbenzonitriles used in training set


Compound	R	Compound	R
39	H	54	2-CN
40	2-OMe	55	3-CN
41	3-OMe	56	4-CN
42	4-OMe	57	3-CF ₃
43	2-Me	58	2,5-Cl ₂
44	3-Me	59	3,5-Cl ₂
45	4-Me	60	3,5-Me ₂
46	2-Cl	61	3-Br, 5-Me
47	3-Cl	62	3-Cl, 5-Me
48	4-Cl	63	3-OMe, 5-Me
49	2-Br	64	3-OMe, 5-CF ₃
50	3-Br	65	3-OH, 5-Me
51	4-Br	66	3-OCH ₂ CH ₃ , 5-Me
52	2-F	67	3-O(CH ₂) ₂ CH ₃ , 5-Me
53	3-F	68	3-O(CH ₂) ₃ CH ₃ , 5-Me

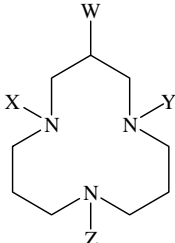
toward the receptor may be measured, and this procedure often provides reliable account for the biological activity of compounds, as compared with experimental data.¹⁷

This work is intended to be a contribution for the treatment of AIDS epidemics, and its main goal was to model potentially active anti-HIV-1 compounds by using the MIA-QSAR procedure and checking the drug-likeness of such ligands by calculating the affinities to the CD4 receptor, which have shown to be linearly related to anti-HIV potency.¹⁸ The new predicted compounds are miscellaneous of substructures of two congeneric sets of anti-HIV-1 compounds, namely 2-amino-6-arylsulfonylbenzonitriles^{3,4} and cyclotriazadisulfonamide analogues.^{18,19}

2. Theoretical calculations

2.1. MIA-QSAR modeling

The MIA-QSAR procedure has been fully described elsewhere,^{15,16} thus only a brief description is given here. The structures of compounds were systematically built using an appropriate software, ChemDraw 7.0,²⁰ and

Table 2. Cyclotriazadisulfonamide analogues used in training set


Compound	X	Y	Z	W
CADA	Ts	Ts	Bz	=CH ₂
QJ023	Ts	Ts	CH ₂ -3-Cyclohexenyl	=CH ₂
QJ027	Ts	Ts	CH ₂ -2-Pyrrolyl	=CH ₂
QJ028	Ts	Ts	CH ₂ -Cyclohexyl	=CH ₂
QJ029	Ts	Ts	CH ₂ CH ₂ CH ₃	=CH ₂
QJ030	Ts	Ts	CH ₂ -4-Pyridinyl	=CH ₂
QJ033	Ts	Ts	COCH ₃	=CH ₂
QJ035	Ts	Ts	CH(CH ₃) ₂	=CH ₂
QJ036	Ts	Ts	2-Butyl	=CH ₂
QJ037	Ts	Ts	CH ₂ -2-Butyl	=CH ₂
QJ038	Ts	Ts	CH ₂ CH ₂ CH(CH ₃) ₂	=CH ₂
QJ040	Ts	Ts	Cyclopentyl	=CH ₂
QJ041	Ts	Ts	CH ₂ -Cyclopropyl	=CH ₂
ASN6P6	Ts	Ts	CH ₂ -3-Pyridinyl	=CH ₂
AS117	Ts	Ts	Bn	CH ₂ Cl
ASPB127	Br	Br	Bn	=CH ₂
95213	Ts	Ts	COOEt	=CH ₂
98035	Ts	Ts	CH ₂ CH(CH ₃) ₂	=CH ₂
HJC321	Ts	Ts	Bn	CH ₂ OH
KKD015	Ts	Dn	Bn	=CH ₂
KKD016	Ts	Dn	CH ₂ C ₆ H ₁₁	=CH ₂
KKD023	SO ₂ -Ph-4-OMe	SO ₂ -Ph-4-OMe	Bn	=CH ₂
KKD025	SO ₂ -Ph-4-OMe	SO ₂ -Ph-4-OMe	H	=CH ₂
KKD027	SO ₂ -Ph-4-OMe	SO ₂ -Ph-4-OMe	CH ₂ CH ₂ CH(CH ₃) ₂	=CH ₂

Ts, tosyl; Bn, benzyl; Dn, danzyl (5-(dimethylamino)-1-naphthalenesulfonyl).

then converted to bitmaps in 733×510 pixels windows, with resolution of 96×96 points per inch. All the molecular structures were fixed by a common point among them in a given coordinate, since the shapes should be superimposed afterward, as a 2D alignment to allow maximum similarity. Each 2D image was read and converted into binaries (double array in Matlab²¹), and the three-way array, the predictors block, was built by grouping the 54 treated images, giving a $54 \times 733 \times 510$ array. The 3D array was unfolded to a 2-way array

($54 \times 373,830$), the **X**-matrix, in order to be correlated with the **Y**-block (the activities column vector) by using the NIPALS algorithm²² for partial least squares (PLS) regression. However, in order to minimize the memory used, columns with zero-variance were removed, reducing the **X** dimension to 54×7791 . The model validation was achieved through leave-one-out cross-validation (LOO CV) and the quality of the results was evaluated by analyzing R^2 and Q_{CV}^2 , the squared correlation coefficients of experimental versus fitted/predicted activities

Table 3. Experimental, fitted, and predicted pIC₅₀, and residuals of calibration and cross-validation

Compound	Experimental	Fitted	Residuals (cal.)	Predicted	Residuals (CV)
39	2.70	2.51	0.19	2.51	0.19
40	3.22	2.31	0.91	2.14	1.08
41	3.05	2.89	0.16	2.86	0.19
42	1.60	2.19	−0.59	2.63	−1.03
43	2.64	2.35	0.29	2.34	0.30
44	3.40	3.24	0.16	3.28	0.12
45	2.02	2.63	−0.61	3.22	−1.20
46	2.39	2.27	0.12	2.29	0.10
47	3.23	3.26	−0.03	3.35	−0.12
48	2.52	2.47	0.05	2.71	−0.19
49	2.30	2.23	0.07	2.27	0.03
50	3.27	2.87	0.40	2.79	0.48
51	1.70	1.99	−0.29	2.29	−0.59
52	2.52	2.29	0.23	2.29	0.23
53	2.52	2.68	−0.16	2.76	−0.24
54	2.27	2.22	0.05	2.27	0.00
55	2.62	2.78	−0.16	2.85	−0.23
56	1.10	1.80	−0.70	2.29	−1.19
57	2.46	2.19	0.27	3.96	−1.50
58	3.52	3.39	0.13	3.25	0.27
59	4.15	4.46	−0.31	4.45	−0.30
60	5.00	4.23	0.77	3.73	1.27
61	4.70	3.99	0.71	3.51	1.19
62	4.52	4.37	0.15	4.21	0.31
63	4.30	4.19	0.11	4.09	0.21
64	4.05	4.28	−0.23	4.13	−0.08
65	3.37	3.99	−0.62	4.04	−0.67
66	4.22	4.20	0.02	4.05	0.17
67	4.22	4.23	−0.01	3.71	0.51
68	3.22	4.27	−1.05	4.47	−1.25
CADA	5.92	5.78	0.14	5.71	0.21
QJ023	6.22	5.93	0.29	5.80	0.42
QJ027	5.10	5.15	−0.05	5.28	−0.18
QJ028	6.54	5.94	0.60	5.74	0.80
QJ029	5.62	5.42	0.20	5.39	0.23
QJ030	5.21	5.66	−0.45	5.84	−0.63
QJ033	5.58	5.16	0.42	5.03	0.55
QJ035	4.98	5.25	−0.27	5.75	−0.77
QJ036	5.45	5.32	0.13	5.31	0.14
QJ037	6.01	5.62	0.39	5.48	0.53
QJ038	6.11	5.58	0.53	5.38	0.73
QJ040	5.19	5.10	0.09	5.13	0.06
QJ041	5.18	5.33	−0.15	5.42	−0.24
ASN6P6	5.25	5.68	−0.43	5.85	−0.60
AS117	5.66	5.72	−0.06	5.24	0.42
ASPB127	5.74	5.65	0.09	3.11	2.63
95213	4.57	5.16	−0.59	5.54	−0.97
98035	4.71	5.44	−0.73	5.63	−0.92
HJC321	5.14	5.65	−0.51	5.69	−0.55
KKD015	5.02	5.34	−0.32	5.72	−0.70
KKD016	5.74	5.51	0.23	5.07	0.67
KKD023	6.21	6.15	0.06	5.68	0.53
KKD025	5.20	5.21	−0.01	5.67	−0.47
KKD027	6.20	5.90	0.30	5.55	0.65

of calibration and validation, respectively. Randomly selected samples, 20% from the total series of 54 compounds, were also used as external test set. Randomization was performed ten times, and an average Q^2 was considered. In addition, the root mean square errors of calibration, cross-validation, and external validation (RMSEC, RMSECV, and RMSEP, respectively) were also used as statistical parameters to give an account for the model predictive ability.

2.2. Docking calculation procedures

Three-dimensional (3D) structures of compounds **QJ028**, **C**, and **D** were built using the PC Spartan program Pro/Builder module.²³ Subsequently, the overall geometry optimizations and partial atomic charge distribution calculations of the ligands were performed with the same program using the AM1 semi-empirical molecular orbital method.²⁴ Crystal coordinates of CD4 enzyme in the bound state with gp120 and 17b were taken from Protein Data Bank (PDB code: 1G9N).²⁵ The compounds were docked into the CD4 binding sites using the Molegro Virtual Docker,²⁶ a program for predicting the most likely conformation of how a ligand will bind to a macromolecule. Ligand molecules and a subset region composed of all amino acid residues having at least one atom within 10 Å of the center of the Phe43 residue are considered flexible during the docking simulation. The MolDock scoring function (MolDock Score) used by Molegro Virtual Docker program is derived from the PLP (Piecewise Linear Potential), a simplified potential whose parameters are fit to protein–ligand structures and binding data scoring functions²⁷ and further extended in GEMDOCK (Generic Evolutionary Method for molecular DOCK) with a new hydrogen bonding term and new charge schemes. The docking scoring function, Escore, is defined by two terms: ligand–protein interaction energy and internal energy of the ligand. The docking search algorithm used in Molegro Virtual Docker is based on interactive optimization techniques inspired by Darwinian evolution theory (evolutionary algorithms—EA). A population of individuals (candidate solutions) is exposed to competitive selection that weeds out poor solutions. Recombination and mutation are used to generate new solutions.^{26,27} The active site exploited in docking studies was defined as a subset region of 10.0 Å around the Phe-43 center. The interaction modes of the ligand with the CD4 active sites were determined as the highest energy scored protein–ligand complex used during docking. We calculated the potential binding sites of CD4 receptor using the built-in cavity detection algorithm from Molegro program.

3. Results and discussion

Two sets of anti-HIV-1 compounds containing a similarity center, an arylsulfonyl moiety, were grouped to compose a training set, in order to be calibrated through PLS regression using the MIA-QSAR (multivariate image analysis applied to QSAR) procedure. Structures were then proposed and their activities predicted using

the calibration model built. Activities were described as the negative logarithm of the concentration of the compound required for 50% reduction of HIV replication (pIC_{50} , IC_{50} in mol L^{-1}). Subsequent docking studies were then carried out for the main proposed compounds against the CD4 receptor. A detailed discussion on these evaluations and strategy is discussed as follows.

3.1. Proposing potential ligands through MIA-QSAR

Geladi and Esbensen²⁸ have demonstrated that image analysis may provide useful information in chemistry, though the descriptors (pixels) do not have a direct physicochemical meaning, since they are binaries. In QSAR, images (2D chemical structures) have shown to contain chemical information,^{15,16} and then the numerous descriptors generated may be treated in a multivariate way in order to correlate the chemical structures with the corresponding dependent variables (bioactivities, pIC_{50}). The key step in the MIA-QSAR modeling is the building of the X-matrix, the predictors block, and performing calibration. Structures of 30 2-amino-6-arylsulfonylbenzonitriles (**39–68**) and 24 cyclotriazadisulfonamides (Tables 1 and 2), obtained from the literature,^{3,4,18,19} were grouped as described in the Theoretical Calculations section, since they are congeners due to a similarity center, a common point among the 2D chemical structures.

Calibration was carried out for the set of 54 compounds using PLS regression. The optimum number of latent variables was reached at 5 PLS components, with RMSEC of 0.40 and the satisfactory R^2 of 0.925. Many explanatory variables may be correlated with target variables using PLS. Depending on the number of latent variables (LVs) used, high correlation coefficients may be obtained using multivariate regressions, even if negligible correlation exists between the two blocks. In order to assure that this is not the case for our modeling, that is, to guarantee that the MIA-QSAR modeling for the anti-HIV compounds did not result from happenstance,

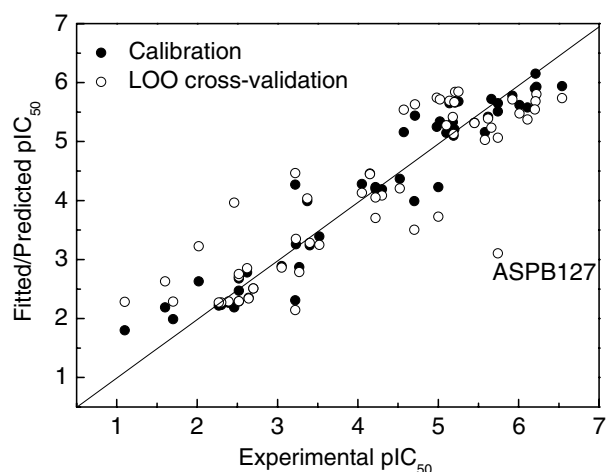


Figure 1. Plot of experimental versus fitted/cross-validated pIC_{50} , using 5 LVs.

the **Y**-block (the activities column vector) was randomized in such a way that compounds were not corresponding to their respective bioactivity values. This procedure gave a R^2 significantly smaller (0.57) than the real R^2 at 5 LVs, confirming that calibration was not a fortuitous correlation and allowing to assess the robustness of the model.

The calibration model built was validated through leave-one-out cross-validation (LOO CV), giving the predicted values of Table 3 and correlation plot of Figure 1. A correlative Q_{CV}^2 of 0.748 (RMSECV = 0.73) was obtained, which is within the range of a validated model ($Q_{CV}^2 > 0.5$).²⁹ However, a cross-validation outlier was identified (compound **ASPB127**), probably due to uncertainty of

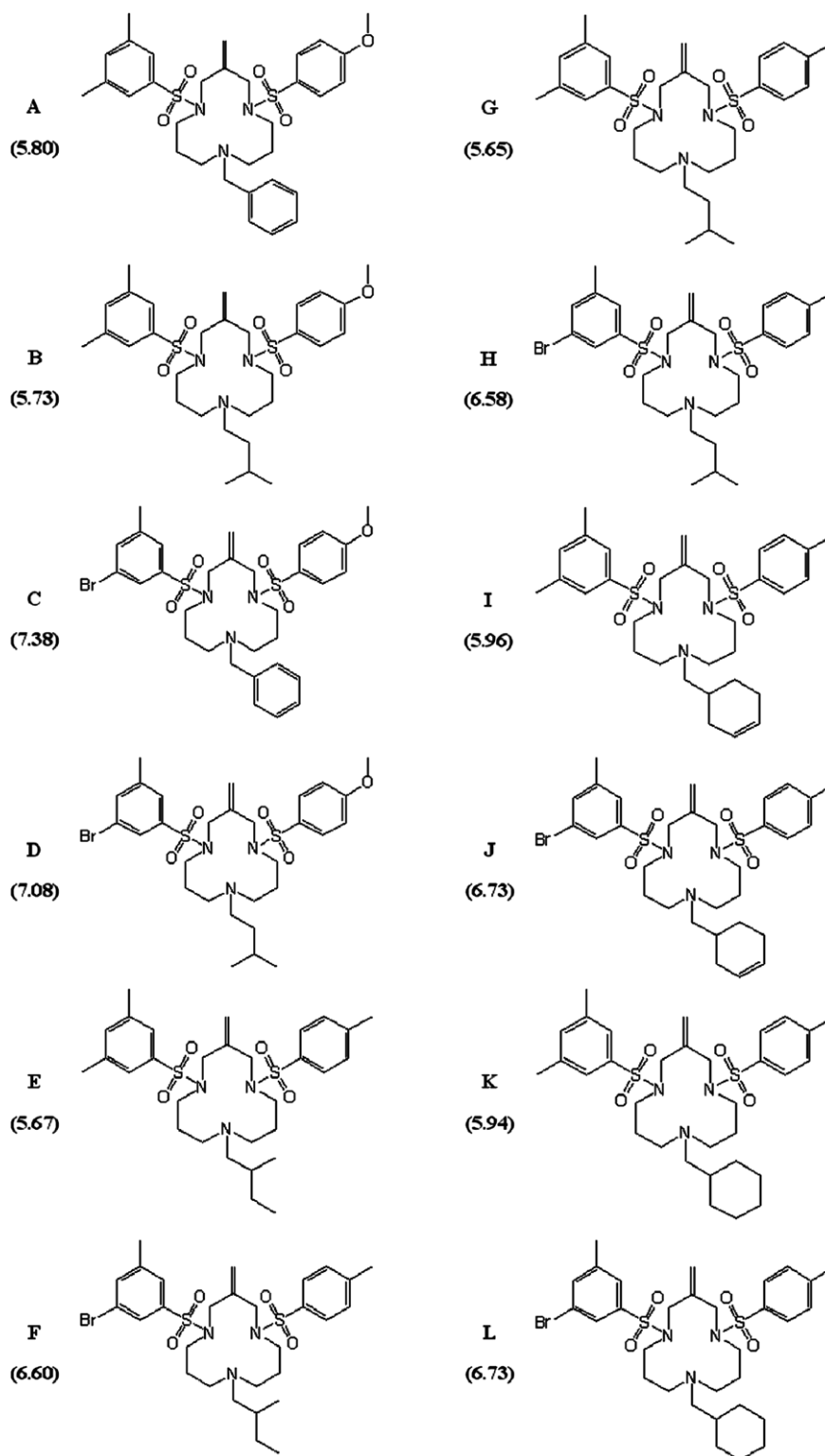


Figure 2. Anti-HIV-1 compounds predicted through MIA-QSAR (pIC_{50} in parentheses).

experimental measurements or, most probably, due to substituent(s) not well calibrated at the respective position(s), as a result of extrapolation. Q_{CV}^2 is improved to 0.805 after removing the cross-validation outlier. LOO CV has often been considered to be an inadequate validation method; external validation has been strongly recommended instead.²⁹ Thus, in order to simulate test sets, the training set was divided into 5 segments (leave-20%-out cross validation). Each segment, composed of 10 or 11 randomly selected samples, was left out, the calibration carried out using the remaining 4 segments, and then the bioactivities for the samples left out predicted using the calculated calibration parameters. This procedure was repeated ten times, resulting in average Q^2 of 0.74 ± 0.02 and RMSEP coincidentally of 0.74 ± 0.02 . Separation of the squared correlation coefficient curves between observed and predicted values with and without intercept was not significant, providing a r_m^2 value close to Q^2 , 0.70 (r_m^2 has been defined elsewhere³⁰ as a term to evaluate external predictability of models; in the best case, $r_m^2 = Q^2$, while in the worst case, $r_m^2 = 0$). Overall, the above results satisfy the recommendation by Golbraikh and Tropsha²⁹ to establish a reliable QSAR model (high Q_{CV}^2 , slope of regression lines through the origin close to 1, and Q_{CV}^2 close to Q^2), and indicate the high external predictability of the QSAR model built, according to Roy and Roy.³⁰

MIA-QSAR has presented the potential of being used as a tool for predicting new drugs, for instance by taking a molecule which is a miscellaneous of substructures of known drugs pertaining to two different congeneric classes having a minimum of similarity. Then, a set of new compounds might be predicted by accounting for the substructures of eight experimentally active compounds of Tables 1 and 2 (60 and 61 from the set of 2-amino-6-aryl-sulfonylbenzonitriles, and QJ023, QJ028, QJ037, QJ038, KKD023, and KKD027 from the set of cyclotriazadisulfonamide analogues). Twelve structures were proposed as shown in Figure 2, and two compounds exhibited especially significant, predicted potency against the HIV virus, C and D (IC₅₀ of 0.04 and 0.08 μ M, respectively), being submitted to docking evaluation.

3.2. Docking evaluation for the predicted anti-HIV compounds

Antiviral activities of a series of cyclotriazadisulfonamide analogues have shown to correlate linearly with the CD4 receptor inhibition.¹⁸ Thus, the binding orientations were studied, and the interaction energy between the CD4 receptor and compounds QJ028, C, and D (Fig. 2) was predicted. Evaluation of the docking results was based on receptor–ligand complementarity, considering steric and electrostatic properties, as well as calculated potential interaction energy in the complex and ligand intramolecular energy. This computational procedure has been successfully applied elsewhere for similar systems.^{17,31}

The potential binding sites of CD4 were calculated and a small cavity of 30.0 Å³ (surface = 96.0 Å²) was observed close to Gln25, Phe26, Hys27, Lys35, Leu37, Gly38,

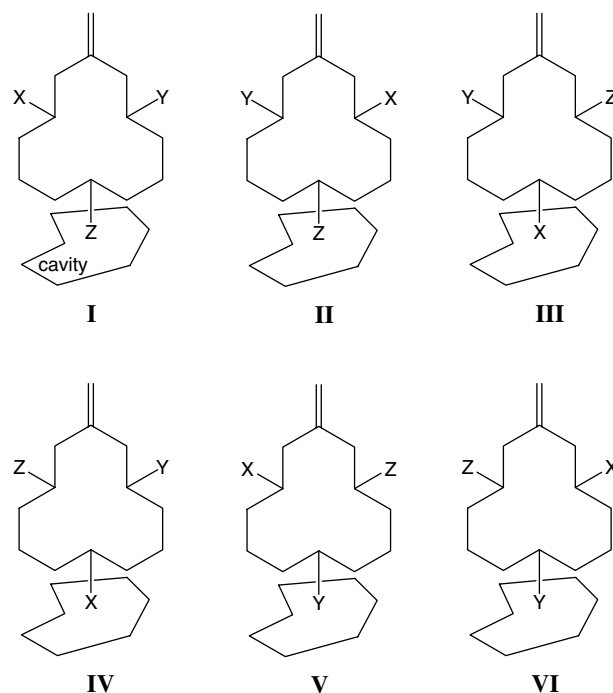


Figure 3. The six conformations (I–VI) obtained for each compound: QJ028, C, and D.

Table 4. Energy score values used for the evaluation of docking poses, total interaction energy between the ligand and receptor, and hydrogen bonding energy between the three inhibitors and CD4 receptor (in kcal mol^{−1})

Compound	Conformation	Energy score	Intermolecular	Hydrogen bonding
QJ028	I = II	−134.81	−147.84	0.0
	III = V	−136.31	−134.86	−4.68
	IV = VI	−131.85	−115.52	−4.68
C	I	—	—	—
	II	—	—	—
	III	−142.43	−136.29	−3.52
	IV	−133.08	−120.11	−2.50
	V	−124.46	−128.72	−2.50
	VI	−133.44	−131.24	−2.48
D	I	−135.70	−133.65	−4.13
	II	—	—	—
	III	−136.49	−130.68	0.0
	IV	−135.11	−127.17	−3.00
	V	−119.64	−121.30	−3.60
	VI	−134.20	−123.39	−0.58

Gln40, and Thr45 residues. In addition, several ligand orientations were produced with one of the aromatic rings inside the cavity, and six conformers (I–VI) were selected, according to Figure 3. Conformations I and II have the substituent Z inside the cavity (Z surrounded by Gln25, Phe26, Hys27, Lys35, Leu37, Gly38, Gln40, and Thr45 residues), whilst the remaining two substituents (Y and X) interact with different amino acids of the active site; conformations III and IV present the X substituent inside the cavity (surrounded by Ser42, Phe43, Leu44, and Gln40 residues), and conformations V and VI, the substituent Y (surrounded by Thr45, Leu46,

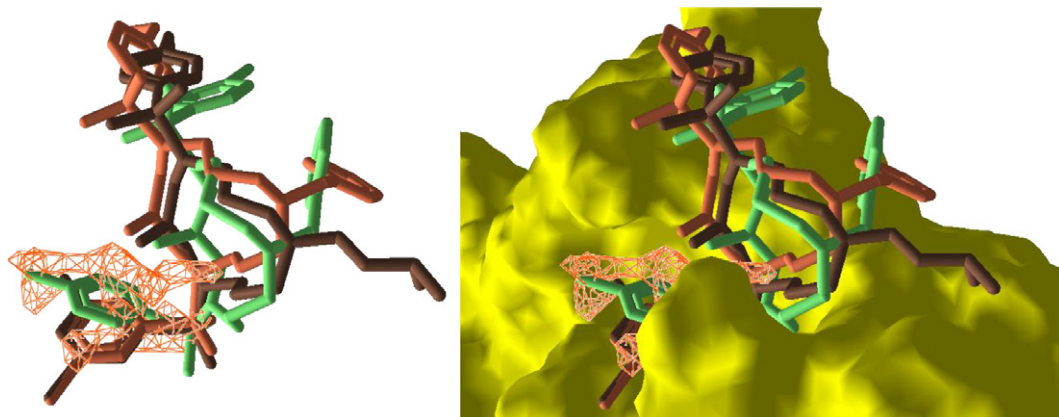


Figure 4. QJ028 (green), C (orange), and D (brown) docked into the cavity of CD4 receptor. On the right, van der Waals surface of the CD4 receptor complexed with the three compounds.

Pro48, and Asn52 residues). The following parameters were then calculated, as shown in Table 4: (a) energy score values used during docking; (b) total interaction energy between ligand and the CD4 receptor; (c) internal energy values of ligand (negligible for all conformations), and (d) hydrogen bonding energy values. Interactions of conformation **III** of compounds QJ028, C, and D with CD4 were more energetically favorable. The structures of the three compounds were superimposed as shown in Figure 4, considering the backbone of CD4 and the van der Waals surface added. Hydrogen bonding was not observed between the CD4 receptor and compounds QJ028 and D. On the other hand, three of such interactions were computed for compound C, in which two of them involved the aromatic ring inside the cavity: one between the sulfonamide oxygen atom and Lys35, and another between the sulfonamide oxygen atom and Thr45 (Fig. 5). Also, the

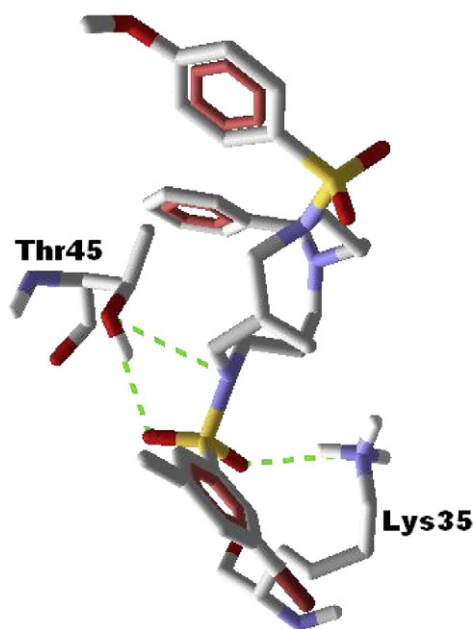


Figure 5. Compound C docked into the active site of CD4 receptor. The residues shown are involved in hydrogen bonding.

nitrogen atom bonded to the X substituent interacts with Thr45, and all of these showed to contribute greatly for the high binding affinity of C toward CD4. An energy score difference of $6.12 \text{ kcal mol}^{-1}$ between the most stable approaches of compounds C and QJ028 (see Table 4) was obtained, resulting in larger predicted activity of compound C when compared to QJ028. Compound D (conformation **III**) exhibited slightly larger affinity to CD4 than QJ028, demonstrating good agreement between the MIA-QSAR results and docking studies.

4. Conclusions

The QSAR method used for modeling anti-HIV compounds showed to be robust, with reliable prediction ability. Given the synergistic effect of some substituents contained in the training set, it was possible to predict novel compounds (miscellaneous of substructures of both classes in training set) with high bioactivity through the MIA-QSAR method, especially C and D (IC_{50} of 0.04 and 0.08 μM , respectively), which were up to 7 times more potent than the reference compound QJ028 ($\text{IC}_{50} = 0.29 \mu\text{M}$). These results were corroborated by docking studies, which revealed the same trend found through the ligand-based approach. Overall, the joint use of MIA-QSAR method and docking studies allowed us to propose at least two highly potent anti-HIV-1 compounds, closely similar to known compounds but with predicted activities largely superior, which are potentially useful in the treatment of AIDS.

Acknowledgments

FAPEMIG is gratefully acknowledged for the support of this research (Grant Nos: CEX 415/06, CEX 353/06, and CEX 97/07), as well as CNPq for a scholarship (M.B.). We are also especially grateful to Dr. Rene Thomsen and Molegro APS for the Molegro Virtual Docker licence.

References and notes

1. 2006 AIDS Epidemic Update (<http://www.unaids.org/en/HIV_data/epi2006/default.asp>).
2. Garg, R.; Gupta, S. P.; Gao, H.; Babu, M. S.; Debnath, A. K.; Hansch, C. *Chem. Rev.* **1999**, *99*, 3525.
3. Leonard, J. T.; Roy, K. *QSAR Comb. Sci.* **2004**, *23*, 23.
4. Roy, K.; Leonard, J. T. *Bioorg. Med. Chem.* **2004**, *12*, 745.
5. Kempf, D. J.; Sham, H. L.; Marsh, K. C.; Flentge, C. A.; Betebenner, D.; Green, B. E.; McDonald, E.; Vasavanonda, S.; Saldivar, A.; Wideburg, N. E.; Kati, W. M.; Ruiz, L.; Zhao, C.; Fino, L.; Patterson, J.; Molla, A.; Plattner, J. J.; Norbeck, D. W. *J. Med. Chem.* **1998**, *41*, 602.
6. Free, S. M.; Wilson, J. W. *J. Med. Chem.* **1964**, *7*, 395.
7. Hansch, C.; Fujita, T. *J. Am. Chem. Soc.* **1963**, *86*, 1616.
8. Todeschini, R.; Consonni, V. In *Handbook of Molecular Descriptors*; Mannhold, R., Kubinyi, H., Timmerman, H., Eds.; Methods and Principles in Medicinal Chemistry; Wiley-VCH, 2000; p 667.
9. Cramer, R. D., III; Patterson, D. E.; Bunce, J. D. *J. Am. Chem. Soc.* **1988**, *110*, 5959.
10. Klebe, G.; Abraham, U.; Mietzner, T. *J. Med. Chem.* **1994**, *37*, 4130.
11. Goodford, P. J. *GRID*; University of Oxford: Oxford, UK, 1995.
12. Hopfinger, A. J.; Wang, S.; Tokarski, J. S.; Jin, B.; Albuquerque, M.; Madhav, P. J.; Duraiswami, C. *J. Am. Chem. Soc.* **1997**, *119*, 10509.
13. Vedani, A.; Dobler, M. *J. Med. Chem.* **2002**, *45*, 2139.
14. Vedani, A.; Dobler, M.; Lill, M. A. *J. Med. Chem.* **2005**, *48*, 3700.
15. Freitas, M. P.; Brown, S. D.; Martins, J. A. *J. Mol. Struct.* **2005**, *738*, 149.
16. Freitas, M. P. *Org. Biomol. Chem.* **2006**, *4*, 1154.
17. da Cunha, E. F. F.; Ramalho, T. C.; de Alencastro, R. B.; Taft, C. A. *Lett. Drug Des. Discov.* **2006**, *3*, 17.
18. Vermeire, K.; Bell, T. W.; Choi, H. J.; Jin, Q.; Samala, M. F.; Sodoma, A.; De Clercq, E.; Schols, D. *Mol. Pharmacol.* **2003**, *63*, 203.
19. Bell, T. W.; Anugu, S.; Mailey, P.; Catalano, V. J.; Dey, K.; Drew, M. G. B.; Duffy, N. H.; Jin, Q.; Samala, M. F.; Sodoma, A.; Welch, W. H.; Schols, D.; Vermeire, K. *J. Med. Chem.* **2006**, *49*, 1291.
20. ChemDraw Ultra 7.0, CambridgeSoft, Cambridge, MA, 1985–2001.
21. Matlab Version 6.5.1, MathWorks Inc., Natick, MA, 1993.
22. Wold, H. In *Multivariate Analysis*; Krishnaiah, K. R., Ed.; Academic Press: New York, 1966; pp 391–420.
23. SpartanPro 1.0.1, Wavefunction, Irvine, CA, 2001.
24. Dewar, M. J. S.; Zoebisch, E. G.; Healy, E. F.; Stewart, J. J. P. *J. Am. Chem. Soc.* **1985**, *107*, 3902.
25. Kwong, P. D.; Wyatt, R.; Majeed, S.; Robinson, J.; R. Sweet, W.; Sodroski, J.; Hendrickson, W. A. *Struct. Fold. Des.* **2000**, *8*, 1329.
26. Thomsen, R.; Christensen, M. H. *J. Med. Chem.* **2006**, *49*, 3315.
27. Gehlhaar, D. K.; Verkhiver, G. M.; Reijto, P. A.; Sherman, C. J.; Fogel, D. B.; Fogel, L. J.; Freer, S. T. *Chem. Biol.* **1995**, *2*, 317.
28. Geladi, P.; Esbensen, K. *J. Chemom.* **1989**, *3*, 419.
29. Golbraikh, A.; Tropsha, A. *J. Mol. Graph. Model.* **2002**, *20*, 269.
30. Roy, P. P.; Roy, K. *QSAR Comb. Sci.* **2007**. doi:10.1002/qsar.200710043.
31. da Cunha, E. F. F.; Ramalho, T. C.; de Alencastro, R. B.; Maia, E. R. *J. Biomol. Struct. Dyn.* **2004**, *22*, 119.